Ginzburg-Landau theory of the upper critical field in filamentary superconductors

L. A. Turkevich*
Department of Physics, Stanford University
Stanford, California 94305

R. A. Klemm
Ames Laboratory (USDOE) and Department of Physics,
Iowa State University, Ames, Iowa 50011
(Received 24 July 1978)

The upper critical field for coupled filamentary superconductors is analyzed within the context of a Ginzburg-Landau theory similar to the Lawrence-Doniach theory for coupled layered superconductors. Upward curvature in the critical field as the temperature is lowered results from the decreased coupling of the filaments, and an ultimate divergence in the critical field at all angles occurs below a decoupling temperature T^*. Unusual anomalies are predicted to occur in the $H_{c2||}(T)$ curve, corresponding to a commensurate fitting of the vortices into the filament lattice. The behavior of H_{c2} for coupled filaments is contrasted with that of an isolated fiber of finite diameter. The model is applied to $(SN)_x$, to the transition-metal trichalcogenides $NbSe_3$ and $TaSe_3$, and to mercury embedded in asbestos.

I. INTRODUCTION

The study of one-dimensional superconductors and their properties has been of interest ever since Little's original proposal[1] that such systems might exhibit high-transition temperatures. The most recent excitonic model[2,3] for such a high-T_c superconductor is also highly one dimensional. Independent of whether such high-T_c materials can ever be made, the quasi-one-dimensional systems are still interesting with regard to their highly anisotropic magnetic field behavior.

Recently, Greene, Street, and Suter[4] have found that crystals of the pseudo-one-dimensional sulphur-nitrogen polymer $(SN)_x$ become superconducting below 0.3 °K. Azevedo *et al.*[5] have since measured the upper critical field for $(SN)_x$ and its angular dependence. This prompts a theoretical investigation of the upper critical field for such filamentary superconductors. In this paper we examine the results of a simple Ginzburg-Landau theory for such systems, analogous to the Lawrence-Doniach theory for layered superconductors.[6] Manneville[7] has independently treated a few special cases of this model, and for these special cases we are in essential agreement with his results. We discuss in detail the application of this model to $(Sn)_x$.[8] More recently, Monceau *et al.*[9,10] have reported a transition under pressure to the superconducting phase in the one-dimensional crystals $NbSe_3$. Sambongi *et al.*[11] have similarly reported a transition to the superconducting phase in $TaSe_3$ at atmospheric pressure. These workers[12,13] have since measured the angular dependence of the upper critical field for $TaSe_3$. Unlike $(SN)_x$, whose fibers contain many microscopic polymer strands, these transition-metal trichalcogenide crystals manifest restricted dimensionality at the microscopic level, and we discuss briefly the application of this model to such systems. Finally we comment on the work of Bogomolov and coworkers, who have successfully manufactured isolated filaments of mercury, embedding the filaments in a matrix of asbestos.[14,15] Their measurements of the critical fields for filaments of various sizes[16,17] are discussed within the context of the proposed model.

The analogy of the coupled filamentary superconductors with the layered superconductors is omnipresent, and it is useful before embarking on details to compare the results of the phenomenological theory for such systems.

For layered superconductors, when a magnetic field is applied perpendicular to the layers, the Cooper pairs form Landau levels within a given layer, and hence, do not feel any interlayer phase difference; thus, there is no Josephson coupling of the layers. The vortex currents circulate freely within the layers [Fig. 1(a)], and the normal vortex cores penetrate all of the layers; the critical-field $H_{c2\perp}$ is essentially that of a bulk superconductor. When, however, a magnetic field is applied parallel to the layers, there is a

phase difference between the layers, and the system behaves as a series of coupled Josephson junctions. The vortex currents partially circulate within the layers but partially tunnel from one layer to the next as Josephson currents [Fig. 1(b)]. The normal vortex cores fit between the layers, and at low temperatures the critical-field $H_{c2\parallel}$ necessary to suppress the superconductivity in the layers markedly exceeds that of a bulk superconductor. As the temperature is reduced well below T_c, the coherence length between layers $\xi_\perp = (m/M)^{1/2}\xi(T)$ decreases, and at a temperature T^* given by $\xi_\perp(T^*) = s/2^{1/2}$ (where s is the layer separation) the layers decouple, and the critical field becomes infinite in the Ginzburg-Landau theory.[18] This divergence of $H_{c2\parallel}$ merely reflects the Ginzburg-Landau result[19] for $H_{c2\parallel}$ of a film with thickness small compared to the penetration depth.

Analogously for filamentary superconductors, when a magnetic field is applied perpendicular to the coupled filaments, there is a phase difference between filaments along one direction, and the system behaves as a series of coupled Josephson junctions. The vortex currents partially circulate along the filaments and partially Josephson tunnel from one filament to the next [Fig. 2(a)]. The normal core can fit between the filaments, and the critical-field $H_{c2\perp}$ exhibits the anomalous behavior characteristic of $H_{c2\parallel}$ for the layered superconductors. In particular, below a temperature T^* the filaments decouple, and the upper critical field diverges in the Ginzburg-Landau theory. This decoupling temperature, at which the coherence length between filaments becomes smaller than the interfilament spacing, is a strong function of azimuthal angle. If the field is imposed along a lattice direction, only the coherence length perpendicular to this direction need become smaller than the lattice spacing; in general, however, when the field is not imposed along a lattice direction, the coherence lengths along *each* lattice direction must decouple. This leads to a lower decoupling temperature for the general perpendicular field than for one applied along a lattice direction. When a magnetic field is applied parallel to the coupled filaments, the vortex currents are entirely Josephson-tunneling currents, the normal vortex cores fitting interstitially in the filament lattice [Fig. 2(b)]. With a parallel applied field, there is a phase difference between filaments in both directions, and the system behaves as a lattice of coupled Josephson junctions—a SQUID (superconducting quantum-interference device) grid. As long as they remain coupled, the filaments cannot discriminate between integral quanta of flux through each SQUID, which results in a periodicity of the critical field at any temperature. As with the perpendicular field, below a certain temperature T^*, the filaments decouple, and no critical field will suppress the superconductivity.

Having established the strong analogy between coupled filamentary and coupled layered superconducting systems, we now examine in some detail the magnetic-field consequences of a phenomenological theory. In Sec. II of this paper we construct a phenomenological Ginzburg-Landau theory for coupled superconducting filaments which is essentially that proposed by Lawrence and Doniach for the layered systems.[6] In Sec. III we discuss the azimuthal dependence of $H_{c2\perp}$. In Sec. IV we discuss the polar dependence of H_{c2} as it is rotated from the perpen-

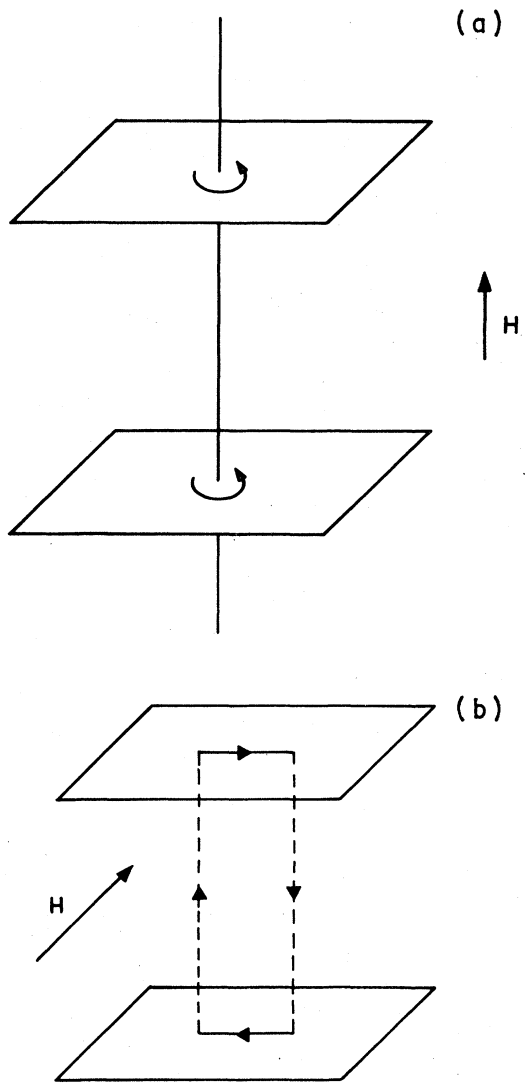

FIG. 1(a). Perpendicular-field $H_\perp$ applied to layered superconductors. The vortex currents circulate within the layers. 1(b). Parallel-field $H_\parallel$ applied to layered superconductors. The vortex currents partially circulate within the layers and partially Josephson tunnel from layer to layer.

dicular to an orientation parallel to the filament direction. For both $H_{c2\perp}$ and $H_{c2\parallel}$ the low-field behavior near T_c is shown to follow an anisotropic mass law. Also both $H_{c2\perp}$ and $H_{c2\parallel}$ are shown to diverge within the model below a temperature T^* at which the filaments decouple. In Sec. V we examine the critical-field behavior of decoupled and hence isolated filaments, taking into account the effect of their finite size. Finally in Sec. VI we apply our model to several physical systems, in some detail to $(SN)_x$, briefly to the transition-metal trichalcogenides $NbSe_3$ and $TaSe_3$, and finally to mercury embedded in asbestos.

II. PHENOMENOLOGICAL GINZBURG-LANDAU MODEL

We consider a rectangular $(a \times b)$ lattice of superconducting filaments oriented in the z direction. We ignore the finite diameter of the filaments. The superconducting order parameter for the ith, jth filament in the (x,y) position on the lattice is denoted by $\psi_j^i(z)$. Following Klemm, Luther, and Beasley,[18] we write the Ginzburg-Landau free energy in gauge-invariant form,

$$F = \int_0^L dz\, ab \sum \left\{ \alpha |\psi_j^i(z)|^2 + \tfrac{1}{2}\beta |\psi_j^i(z)|^4 + \frac{1}{2m} \left| \left(\frac{\hbar}{i}\frac{\partial}{\partial z} - \frac{2e}{c} A_z(\vec{r}) \right) \psi_j^i(z) \right|^2 \right.$$
$$+ \zeta_x |\psi_j^{i+1}(z) \exp\left[\frac{-i2e}{\hbar c} \int_{ia}^{(i+1)a} A_x(\vec{r})\, dx \right] - \psi_j^i(z)|^2$$
$$\left. + \zeta_y |\psi_{j+1}^i(z) \exp\left[\frac{-i2e}{\hbar c} \int_{jb}^{(j+1)b} A_y(\vec{r})\, dy \right] - \psi_j^i(z)|^2 + \frac{1}{8\pi} |\vec{H}(\vec{r}) - \vec{H}_a|^2 \right\} , \quad (1)$$

where

$$\alpha = -\hbar^2/2m\xi^2(T) = \hbar^2/2m\xi^2(0)(T - T_c)/T_c$$

is the usual Ginzburg-Landau parameter, and

$$\zeta_x = \hbar^2/2M_x a^2, \quad \zeta_y = \hbar^2/2M_y b^2$$

are the interchain coupling parameters due to the Josephson tunneling of electron pairs, which expressions define the interchain masses M_x and M_y. The local magnetic-field $\vec{H}(\vec{r})$ is assumed constant and equal to the constant applied magnetic-field

$$\vec{H}_a = H(\sin\theta\sin\phi, \sin\theta\cos\phi, \cos\theta) ,$$

since near H_{c2} the small order parameter cannot ap-

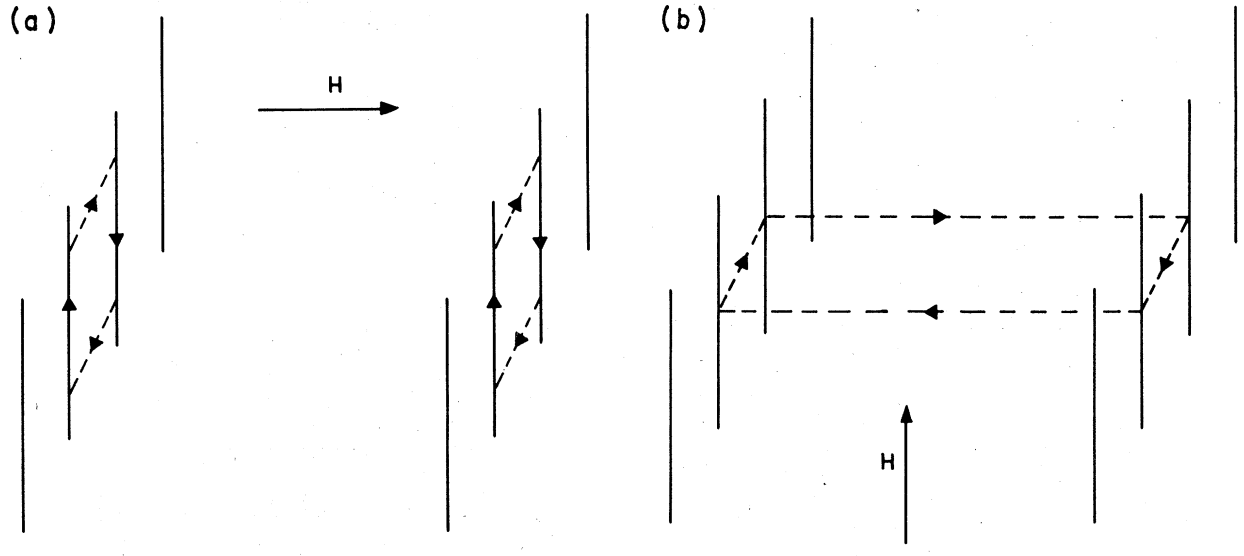

FIG. 2. (a) Perpendicular-field $H_\perp$ applied to filamentary superconductors. The vortex currents partially circulate along the filaments and partially Josephson tunnel from filament to filament. (b) Parallel-field $H_\parallel$ applied to filamentary superconductors. The vortex currents are entirely Josephson tunneling currents.

preciably alter the local field from the applied field. Utilizing the Coulomb gauge, the vector potential is

$$\vec{A} = H[z\sin\theta\cos\phi - \gamma y\cos\theta, \quad (1-\gamma)x\cos\theta - z\sin\theta\sin\phi, 0] \ , \qquad (2)$$

where the parameter γ reflects the only remaining gauge freedom.

We demand that the free energy be a minimum with respect to functional variations in $\psi_l^k(z)$ *. Due to the Josephson coupling of the filaments, the system is actually three-dimensional above T^*; interfilament phase fluctuations are assumed not to destroy the long-range order generated by this minimization of the free energy. Neglecting the term $\beta|\psi_l^k|^2\psi_l^k$, which will be small near the phase boundary, we obtain the linearized Ginzburg-Landau equations

$$\left(\alpha - \frac{\hbar^2}{2m}\frac{d^2}{dz^2} + 2\zeta_x + 2\zeta_y\right)\psi_l^k(z) - \zeta_x\left[\exp\left(\frac{i2h}{d^2}a(z\sin\theta\cos\phi - \gamma lb\cos\theta)\right)\psi_l^{k-1} + \exp\left(\frac{-i2h}{d^2}a(z\sin\theta\cos\phi - \gamma lb\cos\theta)\right)\psi_l^{k+1}\right] - \zeta_y\left[\exp\left(\frac{i2h}{d^2}b[(1-\gamma)ka\cos\theta - z\sin\theta\sin\phi]\right)\psi_{l-1}^k + \exp\left(\frac{-i2h}{d^2}b[(1-\gamma)ka\cos\theta - z\sin\phi]\right)\psi_{l+1}^k\right] = 0 \ , \qquad (3)$$

where we have defined a (dimensionless) reduced field $h = eHd^2/\hbar c$ and the length

$$d = (a^2\cos^2\phi + b^2\sin^2\phi)^{1/2} \ .$$

This is a set of periodically coupled one-dimensional Schrödinger equations. No value of γ (i.e., no choice of gauge) successfully decouples these equations for $\theta \neq 0, \frac{1}{2}\pi$.

To calculate H_{c2} we set $-\alpha$ equal to the lowest eigenvalue of the system (3), thereby determining the highest field for which a nontrivial order parameter exists. Physically, the solutions of Eq. (3) can be characterized as belonging to two-temperature regimes. Near T_c the correlation length $\xi_\perp(T)$ is large compared to the filament spacing, and the coupled filamentary system behaves as an anisotropic superconductor with the critical field given by an anisotropic mass formula. Below the decoupling temperature T^* the correlation length $\xi_\perp(T)$ becomes smaller than the filament spacing, and the system behaves as a collection of decoupled filaments with the critical field enhanced over its bulk value by the small size of the filaments. In our model we have neglected any size to the filaments, and the critical field thus diverges at T^*.

III. AZIMUTHAL DEPENDENCE OF $H_{c2\perp}$

We impose the magnetic field perpendicular to the filament direction ($\theta = \frac{1}{2}\pi$) and investigate the azimuthal dependence of $H_{c2\perp}(T, \phi)$, i.e.,

$$\alpha\psi_l^k - \frac{\hbar^2}{2m}\frac{d^2\psi_l^k}{dz^2} + \zeta_x\left[2\psi_l^k - \exp\left(\frac{i2h}{d^2}az\cos\phi\right)\psi_l^{k-1} - \exp\left(\frac{-i2h}{d^2}az\cos\phi\right)\psi_l^{k+1}\right] + \zeta_y\left[2\psi_l^k - \exp\left(\frac{-i2h}{d^2}bz\sin\phi\right)\psi_{l-1}^k - \exp\left(\frac{i2h}{d^2}bz\sin\phi\right)\psi_{l+1}^k\right] = 0 \ . \qquad (4)$$

All dependence on the gauge parameter γ has vanished. Furthermore the Ginzburg-Landau equations decouple in the sense that the k and l dependence in the exponentials has also vanished. Fourier transforming with respect to the chain indices yields a one-dimensional Schrödinger equation with two periodic potentials,

$$-\frac{\hbar^2}{2m}\frac{d^2\psi}{dz^2} + 2\zeta_x\left[1 - \cos\left(\frac{2h}{d^2}az\cos\phi - Q_x a\right)\right]\psi + 2\zeta_y\left[1 - \cos\left(\frac{2h}{d^2}bz\sin\phi - Q_y b\right)\right]\psi = -\alpha\psi = E\psi \ . \qquad (5)$$

The lowest eigenvalue occurs for $Q_x = Q_y = 0$.

Equation (5) is a two-term Hill equation and is typical of the eigenvalue problem encountered in band theory. The tight-binding approximation (large ζ_x, ζ_y) corresponds in this situation to the small field regime ($H \to 0$ near T_c); the nearly-free-electron approximation (small ζ_x, ζ_y) corresponds in this situation to the large field regime ($H \to \infty$ near T^*). As in band theory, to find the energy E as a general function of the potential parameters is difficult, so in this situation to generate the critical-field curve $H_{c2}(T)$ for all temperatures and orientations is nontrivial. Two special cases ($\phi = 0$ and $\phi = \frac{1}{4}\pi$ for the isotropic system) may be solved exactly, and this is treated in Appendix A. We discuss in the remainder of this section the high- and low-field approximations for arbitrary azimuthal angle ϕ.

For small magnetic-fields
$H \ll (m/M_x)^{1/2}(\Phi_o/\pi a^2)$ and
$H \ll (m/M_y)^{1/2}(\Phi_0/\pi b^2)$, (where $\Phi_0 = hc/2e$ is the flux quantum) the cosines may be expanded to give a simple-harmonic-oscillator equation

$$\frac{-\hbar^2}{2m}\frac{d^2\psi}{dz^2} + \frac{\hbar^2}{2}\left(\frac{2h}{d}\right)^2\left(\frac{\cos^2\phi}{M_x} + \frac{\sin^2\phi}{M_y}\right)z^2\psi = E\psi \quad . \tag{6}$$

Inverting the lowest eigenvalue yields the expected anisotropic Ginzburg-Landau result

$$H_{2c\perp}(T,\phi) = \frac{\Phi_0}{2\pi\xi^2(0)}\left|\frac{T-T_c}{T_c}\right|\left(\frac{m}{M_x}\cos^2\phi + \frac{m}{M_y}\sin^2\phi\right)^{-1/2} \quad . \tag{7}$$

Keeping higher-order terms in the expansion of the cosines, we may generate by perturbation theory an expansion for $H_{c2\perp}$ in powers of $|(T-T_c)/T_c|$,

$$H_{c2\perp}(T,\phi) = \frac{\Phi_0}{2\pi\xi^2(0)}\left|\frac{T-T_c}{T_c}\right|\left(\frac{m}{M_x}\cos^2\phi + \frac{m}{M_y}\sin^2\phi\right)^{-1/2}\sum_{n=0} a_n(\phi)\left|\frac{T-T_c}{T_c}\right|^n \quad . \tag{8}$$

For the case of isotropic coupling [$\zeta_x = \zeta_y$; $\xi_\perp^2 = m/M\xi^2(0)$] we find these coefficients to be

$$\begin{aligned} a_0 &= 1 \quad , \\ a_1 &= \left(\frac{a}{4\xi_\perp^2}\right)^2(\cos^4\phi + \sin^4\phi) \quad , \\ a_2 &= \left(\frac{a}{4\xi_\perp^2}\right)^4\left[\tfrac{13}{3}(\cos^4\phi + \sin^4\phi)^2\right. \\ &\qquad \left. -\tfrac{4}{3}(\cos^6\phi + \sin^6\phi)\right] \quad . \end{aligned} \tag{9}$$

For the angles $\phi = 0, \frac{1}{4}\pi$ these coefficients reduce (to the order calculated) to the exact results given in Appendix A. It should be noted that there is weak azimuthal dependence to the critical field even for an isotropic lattice. Since, to second order, all the coefficients a_n are positive, the critical field $H_{c2\perp}$ is given upward curvature as the temperature is lowered. This curvature becomes significant only for $a/4\xi_\perp \sim 1$, i.e., for $T \sim T^*$. The upward curvature results from the filaments decoupling as the temperature is lowered and is in marked contrast with the result (46) for isolated filaments.

For large magnetic fields the cosine potentials oscillate wildly, and the Schrödinger wave function can easily tunnel through the potential barriers. The eigenfunctions are plane waves $e^{ik_z z}$, and the lowest eigenvalue occurs for $k_z = 0$. This defines a temperature T^* at which $H_{c2\perp}$ becomes infinite, i.e.,

$$T^*/T_c = \begin{cases} 1 - 2\dfrac{m\xi^2(0)}{M_x a^2}, & \phi = 0 \quad , \\ 1 - 2\dfrac{m\xi^2(0)}{M_y b^2}, & \phi = \frac{1}{2}\pi \quad , \\ 1 - 2\left(\dfrac{m\xi^2(0)}{M_x a^2} + \dfrac{m\xi^2(0)}{M_y b^2}\right) & \quad . \end{cases} \tag{10}$$

Since the temperature T^* differs for $\phi = 0$ and $\phi = \frac{1}{2}\pi$ from the other angles, we expect, without further analysis, that there will be strong angular dependence of $H_{c2\perp}$ near the lattice directions for temperatures well below T_c. The actual divergence of $H_{c2\perp}$ is the artifact (46) of our having set the filament size to zero and of our neglect of depairing effects.

At $\phi = 0$ (or $\phi = \frac{1}{2}\pi$ with M_x and a replaced by M_y and b, respectively), one of the cosine potentials ceases to oscillate, and the Schrödinger equation becomes (with the change of variable $x = zh/a$),

$$\frac{d^2\psi}{dx^2} - \frac{1}{h^2}\left(2\frac{m}{M_x} + \frac{a^2}{\xi^2(0)}\frac{T-T_c}{T_c}\right)\psi + \frac{2m}{M_x}\frac{1}{h^2}\cos(2x)\psi = 0 \quad . \tag{11}$$

This is just the Mathieu equation. The small parameter (large h) expansion for the lowest eigenvalue is well known[20] and may be inverted to give

$$H_{c2\perp}(T,\phi=0)\cong\frac{\Phi_0}{2\pi a^2}\frac{m}{2^{1/2}M_x}\times\left[\frac{1}{\xi^2(0)}\frac{T-T_c}{T_c}+\frac{2m}{M_x a^2}\right]^{-1/2}, \quad (12)$$

which diverges at the temperature

$$\frac{T^*}{T_c}=1-2\frac{m\xi^2(0)}{M_x a^2} .$$

This result for the perpendicular critical field along a lattice direction was obtained by Manneville.[7] However, as indicated by Eq. (10), the high-field behavior is considerably more complex, as the general $H_{c2}(\phi)$ diverges at a lower T^*.

To pursue the high-field expansion analytically for arbitrary ϕ, we assume without loss of generality[21] that the arguments of the cosine potentials are commensurate

$$\frac{a\cos\phi}{d}=\frac{n_x}{N}, \quad \frac{b\sin\phi}{d}=\frac{n_y}{N}, \quad (13)$$

for some integers n_x, n_y, N. Changing the independent variable to $x=hz/Nd$ and redefining the coupling parameters

$$\sigma_x=\frac{2md^2}{\hbar^2}\zeta_x, \quad \sigma_y=\frac{2md^2}{\hbar^2}\zeta_y, \quad (14)$$

the Schrödinger equation takes the form of a two-term Hill equation[22]

$$\frac{d^2\psi}{dx^2}+\sigma^2\psi+2\lambda(\sigma_x\cos 2n_x x+\sigma_y\cos 2n_y x)\psi=0 , \quad (15)$$

where the eigenvalue is

$$\sigma^2=\lambda\epsilon=-\lambda(2md^2/\hbar^2)(\alpha+2\zeta_x+2\zeta_y) . \quad (16)$$

We will attempt to construct a perturbation expansion for the eigenvalue in powers of the small parameter $\lambda=N^2/h^2$.

Floquet theory[23,24] (which is just a manifestation of Bloch's theorem) suggests we look for solutions of the form[21]

$$\psi(x)=e^{i\tau x}\left[a_0+\sum_k a_k e^{i(p_k n_k+q_k n_y)x}\right], \quad (17)$$

where τ is a complex number, and p_k and q_k are integers. Substituting the form (17) into the differential Eq. (15) yields a system of linear algebraic equations for the coefficients a_k. This system will possess a nontrivial solution provided that the secular determinant vanishes. The secular determinantal equation may be rearranged[21] into the form

$$\sigma^2+\sum_{(\kappa_l)}\lambda^{j+1}\frac{\sigma_{|\kappa_1|}\cdots\sigma_{|\kappa_j|}\sigma_{|\kappa_1+\cdots+\kappa_j|}}{[(2\kappa_1+\tau)^2-\sigma^2][(2\kappa_1+2\kappa_2+\tau)^2-\sigma^2]\cdots[(2\kappa_1+2\kappa_2+\cdots+2\kappa_j+\tau)^2-\sigma^2]}=0 , \quad (18)$$

where the sum is over all $\kappa_l=n_x$, n_y subject to the restrictions $\kappa_1+\cdots+\kappa_j=\pm n_x,\pm n_y$ and $\kappa_1\pm\cdots\pm\kappa_i\neq 0$ for all $i<j$. This is a power series in $\lambda\sim 1/H^2$ and hence, will serve as the desired high-field expansion. The lowest eigenvalue occurs for $\tau=0$, i.e., for a purely periodic wave function.

For ϕ sufficiently far from 0 and $\frac{1}{2}\pi$ there are no problems with vanishing denominators. Working to lowest order, we have

$$\lambda\epsilon+2\lambda^2\frac{\sigma_{n_x}^2}{2n_x^2-\lambda\epsilon}+2\lambda^2\frac{\sigma_{n_y}^2}{4n_y^2-\lambda\epsilon}+O(\lambda^3)=0 . \quad (19)$$

Absorbing the λ dependence in the denominators into $O(\lambda^3)$ and inverting for $1/\lambda\sim H^2$ we obtain

$$H_{c2\perp}(T,\phi)=\frac{\Phi_0}{2\pi d^2}\frac{1}{2^{1/2}}\left|\left[\left(\frac{md^2}{M_x a^3\cos\phi}\right)^2+\left(\frac{md^2}{M_y b^3\sin\phi}\right)^2\right]\Big/\left[\frac{1}{\xi^2(0)}\frac{T-T_c}{T_c}+2\left(\frac{m}{M_x a^2}+\frac{m}{M_y b^2}\right)\right]\right|^{1/2} , \quad (20)$$

which diverges at the temperature

$$T^*/T_c=1-2[m\xi^2(0)/M_x a^2+m\xi^2(0)/M_y b^2] .$$

It also exhibits the anticipated singular behavior as ϕ approaches 0 and $\frac{1}{2}\pi$. It should be noted that at $\phi=\frac{1}{4}\pi$ for isotropic coupling, Eq. (20) underestimates the exact results of Appendix A by a factor of $2^{1/2}$, although Eq. (20) correctly identifies T^*. As discussed in Appendix C an infinite series again must be summed for this special angle.

In Appendix B we examine the behavior of $H_{c2\perp}$ in the vicinity of $\phi=0$. As we let $\phi\to 0$ (i.e., $n_y\to 0$), the high-field expansion (18) contains divergent terms to all orders in λ. The series of divergent terms is summed in Appendix C, yielding a tractable expression for $H_{c2\perp}$ near $\phi=0$. The singularity at $\phi=0$ manifests itself in the change in order of the resulting eigenvalue equation for the critical field, which diverges at a spurious T^* for this special angle. The behavior of $H_{c2\perp}(T)$ for various azimuthal angles is graphed in Fig. 3 for the special case of isotropic coupling. The very strong azimuthal dependence near $\phi=0$ should be noted.

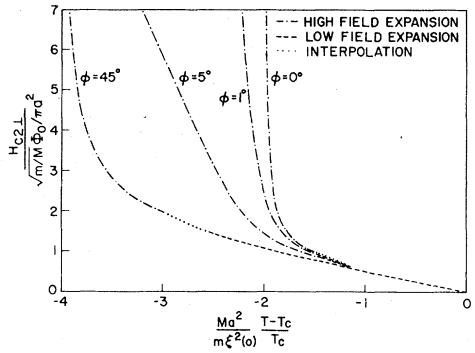

FIG. 3. Perpendicular critical-field $H_{c2\perp}(T)$ for various azimuthal angles. There is pronounced azimuthal dependence near the lattice direction ($\phi=0°$).

IV. POLAR DEPENDENCE OF $H_{c2\parallel}$

We first impose the magnetic field parallel to the filament direction ($\theta=0$) and investigate the temperature dependence of $H_{c2\parallel}$. The Ginzburg-Landau equations no longer decouple. By choice of gauge $\gamma=0$ we may eliminate the l dependence from the exponentials, and the remaining l dependence in the indices may be Fourier transformed away. The lowest eigenvalue occurs for $Q_y=0$,

$$\left(\alpha-\frac{\hbar^2}{2m}\frac{d^2}{dz^2}+2\zeta_x+2\zeta_y\right)\psi_0^k-\zeta_x(\psi_0^{k-1}+\psi_0^{k+1}) -2\zeta_y\cos\left(\frac{2h}{d^2}bka\right)\psi_0^k=0 \quad . \tag{21}$$

The lowest eigenvalue occurs for $\tau=0$.

This is a transcendental equation for the eigenvalues ϵ, analogous to the well-known[26] continued-fraction equation for the Mathieu eigenvalues. It must be solved in some approximation for $\epsilon(\chi)$, i.e., for $\epsilon(H)$ and then inverted to give $H_{c2\parallel}$ as a function of temperature. When this is done numerically, we obtain the temperature dependence of $H_{c2\parallel}$ shown in Fig. 4. The low-field behavior of $H_{c2\parallel}$ is in agreement with the numerical results of Manneville.[7] Since the continued fraction is a periodic function of

The z dependence may be taken to be plane wave $e^{ik_z z}$, with the lowest eigenvalue having $k_z=0$. Setting $\chi=2hab/d^2$ and $\epsilon=\alpha+2\zeta_x+2\zeta_y$ the coupled Schrödinger equations become a pure difference equation,

$$[\epsilon-2\zeta_y\cos(k\chi)]\psi^k-\zeta_x(\psi^{k-1}+\psi^{k+1})=0 \quad . \tag{22}$$

This is a periodic finite difference system analogous to the Mathieu differential equation. We observe immediately that ϵ is periodic in the parameter χ, and hence the phase boundary between the normal and superconducting states is periodic in the critical field. By the difference equation analog of Floquet's theorem,[25] this system admits solutions of the form

$$\psi^k=e^{i\tau k}\sum_{n=0}^{\infty}a_n\cos(nk\chi) \quad . \tag{23}$$

Substituting Eq. (23) into the Eq. (22) and equating coefficients of $\cos(mk\chi)$ yields

$$\begin{aligned}
&\epsilon a_0=\zeta_y a_1+2\zeta_x\cos\tau a_0 \quad ,\\
&\epsilon a_1=2\zeta_y a_0+\zeta_y a_2+2\zeta_x\cos\tau\cos\chi a_1 \quad ,\\
&\epsilon a_n=\zeta_y(a_{n-1}-a_{n+1})+2\zeta_x\cos\tau\cos n\chi a_n \quad n>1 \quad .
\end{aligned} \tag{24}$$

These relations may be combined into a continued fraction equation for the eigenvalues,

$$\epsilon-2\zeta_x\cos\tau-\cfrac{2\zeta_y^2}{\epsilon-2\zeta_x\cos\tau\cos\chi-\cfrac{\zeta_y^2}{\epsilon-2\zeta_x\cos\tau\cos2\chi-\cfrac{\zeta_y^2}{\epsilon-2\zeta_x\cos\tau\cos3\chi-\cdots}}}=0 \tag{25}$$

χ (i.e., of H), the roots of the continued-fraction equation (25) are also periodic in H. This is dramatically reflected in the inverse-periodic behavior of $H_{c2\parallel}(T)$ as shown in Fig. 4. Neither this strict inverse periodicity of $H_{c2\parallel}(T)$ nor its origin was explored by Manneville. Physically, each repetition in Fig. 4 corresponds to an additional flux quantum being put through each unit cell of the lattice of filaments. Since for parallel fields the coupled filaments act as a grid of Josephson junctions, they cannot discriminate between different fields modulo a flux

quantum. The additional structure in the $H_{c2\|}(T)$ curve occurs as fractional flux quanta are put through each unit cell of the lattice of filaments. This is equivalent to integral flux quanta being put through larger unit cells of the lattice of filaments. In other words, the system "resonates" in the critical-field curve whenever an integral number of flux quanta are put through a SQUID of the lattice, where the SQUID size may be any integral number of lattice unit cells, but where the largest resonance occurs for the unit-cell SQUID.

For small-fields $H \ll (m/M_x)(\Phi_0/\pi a^2)$, the cosine of the angle χ may be expanded, and the continued fraction rearranged to

$$\epsilon-2\zeta_x-\cfrac{2\zeta_y^2}{\epsilon-2\zeta_x+1^2(\zeta_x\chi^2)-\cfrac{\zeta_y^2}{\epsilon-2\zeta_x+2^2(\zeta_x\chi^2)-\cfrac{\zeta_y^2}{\epsilon-2\zeta_x+3^2(\zeta_x\chi^2)-\cdots}}}=0\ , \tag{26}$$

which is just the continued-fraction equation for the Mathieu eigenvalue[26] $-4(-2\zeta_x/\zeta_x\chi^2)$ with parameter $4\zeta_y/\zeta_x\chi^2$. Physically, in this low-field regime the vector potential does not vary appreciably from filament to filament; the magnetic field is not sensitive to the discrete nature of the filament system, and hence mathematically the discrete difference system reduces to the continuous differential equation. In the large parameter limit the Mathieu eigenvalue is given by[27]

$$-4\frac{\epsilon-2\zeta_x}{\zeta_x\chi^2}=-2\frac{4\zeta_y}{\zeta_x\chi^2}+2\left(\frac{4\zeta_y}{\zeta_x\chi^2}\right)^{1/2}-\frac{1}{4}+\cdots\ . \tag{27}$$

This may be inverted to give the parallel critical field near T_c. For isotropic coupling (where $a=b$) we have

$$H_{c2\|}(T)=\frac{\Phi_0}{2\pi\xi^2(0)}\left|\frac{T-T_c}{T_c}\right|\frac{M}{m}\times\left[1+\frac{1}{16}\frac{a^2}{\xi^2(0)}\frac{M}{m}\left|\frac{T-T_c}{T_c}\right|+\cdots\right]\ . \tag{28}$$

There is again upward curvature in $H_{c2\|}$ as the temperature is lowered, percentagewise identical to the upward curvature Eq. (19) in $H_{c2\perp}$ for $\phi=0$ or $\phi=\frac{1}{2}\pi$. Again the tendency to decouple produces upward curvature and should be contrasted with the downward curvature exhibited in Eq. (46) by an isolated filament.

For the parallel critical field, the minimum extrusion of the phase boundary can be located on Fig. 4 as being given by

$$\frac{Ma^2}{m\xi^2(0)}\frac{T_{\|}^{\min}-T_c}{T_c}\cong-1.4\ . \tag{29}$$

Below this temperature there is never a normal phase, and hence only an infinite critical field will suppress the superconductivity in the filaments. This is not, however, the decoupling temperature T^*, which can be obtained by taking the $H\to\infty$ limit of Eq. (3) for arbitrary angle, and which is found to be given by Eq. (10). This divergence of $H_{c2\|}$ again reflects the result of our having set the filament size to zero [Eq. (46)].

We now examine the polar dependence of the critical magnetic field near T_c. By choice of gauge $\gamma=0$ we may eliminate the l dependence from the exponentials, and the remaining l dependence in the indices may be Fourier transformed away. The lowest eigenvalue occurs for $Q_y=0$. We consider azimuthal angle $\phi=\frac{1}{2}\pi$ where $d=b$ (the analysis for $\phi=0$ is identical with the alternate choice of gauge $\gamma=1$, where $d=a$). We have

$$\left[\alpha-\frac{\hbar^2}{2m}\frac{d^2}{dz^2}+2\zeta_x+2\zeta_y\right]\psi_0^k-\zeta_x(\psi_0^{k-1}+\psi_0^{k+1})-2\zeta_y\cos\left[\frac{2h}{b}(ka\cos\theta-z\sin\theta)\right]\psi_0^k=0\ . \tag{30}$$

For small fields the vector potential does not vary appreciably from filament to filament. The order parameter thus varies only slightly from filament to filament and may be expanded (setting $x=ka$),

$$\psi(z,x\pm a)=\psi(z,x)\pm a\frac{\partial\psi(z,x)}{\partial x}+\frac{1}{2}a^2\frac{\partial^2\psi(z,x)}{\partial x^2}\ . \tag{31}$$

Substituting Eq. (31) into Eq. (30) yields

$$\left[\alpha-\frac{\hbar^2}{2m}\frac{\partial^2}{\partial z^2}+2\zeta_y-\zeta_x a^2\frac{\partial^2}{\partial x^2}\right]\psi(z,x)-2\zeta_y\cos\left[\frac{2h}{b}(x\cos\theta-z\sin\theta)\right]\psi(z,x)=0\ . \tag{32}$$

Changing variables to

$$\bar{z}=x\sin\theta+z\cos\theta,\quad \bar{x}=x\cos\theta-z\sin\theta\ , \tag{33}$$

the differential equation becomes (dropping the bars),

$$(\alpha+2\zeta_y)\psi-\tfrac{1}{2}\hbar^2\left[\frac{\sin^2\theta}{m}+\frac{\cos^2\theta}{M_x}\right]\frac{\partial^2}{\partial x^2}-\hbar^2\sin\theta\cos\theta\left[\frac{1}{M_x}-\frac{1}{m}\right]\frac{\partial^2\psi}{\partial x\,\partial z}-\tfrac{1}{2}\hbar^2\left[\frac{\cos^2\theta}{m}+\frac{\sin^2\theta}{M_x}\right]\frac{\partial^2\psi}{\partial z^2}$$
$$-\frac{\hbar^2}{2M_y b^2}\cos\left[\frac{2hx}{b}\right]\psi=0\ . \tag{34}$$

Since the potential is now independent of z we may assume plane-wave states in this variable, $e^{ik_z a}$. The lowest eigenvalue occurs for $k_z=0$, and we recover the Mathieu equation. Since this is a low-field expansion, we may also expand the cosine potential to obtain the simple-harmonic-oscillator equation

$$-\frac{\hbar^2}{2m}\left[\frac{\sin^2\theta}{m}+\frac{\cos^2\theta}{M_x}\right]\frac{\partial^2\psi}{\partial x^2}+\frac{\hbar^2}{2M_y}\left[\frac{2h}{d^2}x\right]^2\psi$$
$$=-\alpha\psi=E\psi\ . \tag{35}$$

Inverting the expression for the lowest eigenvalue yields the expected anisotropic Ginzburg-Landau result

$$H_{c2}(T,\theta,\phi=\tfrac{1}{2}\pi)=\frac{\Phi_0}{2\pi\xi^2(0)}\left|\frac{T-T_c}{T_c}\right|\left[\frac{M_y}{m}\right]^{1/2}$$
$$\times\frac{1}{[\sin^2\theta+(m/M_x)\cos^2\theta]^{1/2}}\ . \tag{36}$$

This polar dependence is plotted in Fig. 5 for various mass ratios m/M.

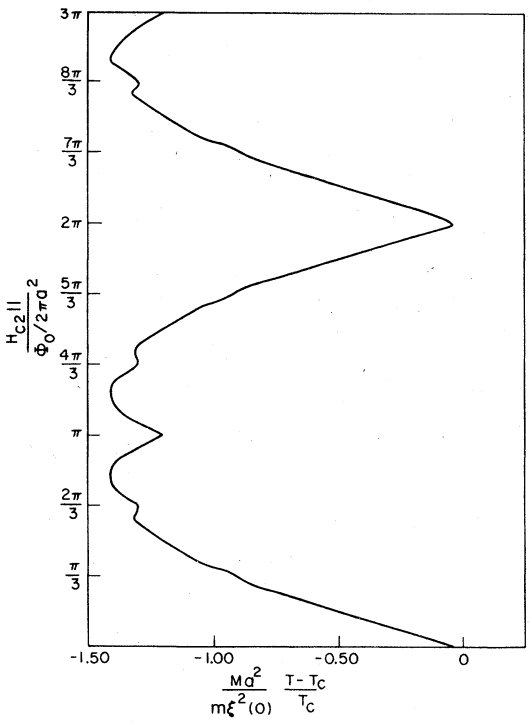

FIG. 4. Parallel critical-field $H_{c2\parallel}(T)$. This is periodic in H every time one flux quantum is put through the lattice of filaments. The additional resonant bumps occur when a flux quantum is put through a larger unit cell of the filament lattice.

V. H_{c2} FOR DECOUPLED FILAMENTS

In this section we discuss the critical-field behavior for decoupled and hence isolated filaments. The divergence of the critical-field $H_{c2\perp}$ and $H_{c2\parallel}$ at T^* in the Lawrence-Doniach model reflects the proportionality of H_{c2} to $1/R$ where R is the filament radius. This finite size was neglected in our earlier treatment of the coupled filaments. Our discussion in this section closely parallels that of Saint-James and Sarma[28] for thin films.

For an isolated filament of radius R the Ginzburg-Landau free energy is given by

$$F=\int_0^L dz\int_0^R r\,dr\int_0^{2\pi} d\chi\left[\alpha|\psi|^2+\tfrac{1}{2}\beta|\psi|^4+\frac{1}{2m^*}\left|\left(\frac{\hbar}{i}\vec{\nabla}-\frac{2e}{c}\vec{A}\right)\psi\right|^2+\frac{h^2}{8\pi}\right] . \tag{37}$$

Choosing a different gauge than in Sec. II, we have

$$\vec{A}=(A_r,A_\chi,A_z)=Hr\left(0,\tfrac{1}{2}\cos\theta,\sin\theta\sin(\chi-\phi)\right) . \tag{38}$$

The boundary condition that there be no supercurrent across the filament surface reduces to

$$\frac{\partial\psi}{\partial r}\Big|_{r=R}=0 . \tag{39}$$

Since the system is really three dimensional due to the finite radius R of the filament, we may functionally vary $\delta\psi^*$ to arrive at the linearized Ginzburg-Landau equation. We have

$$-\frac{\hbar^2}{2m^*}\left(\frac{\partial^2\psi}{\partial r^2}+\frac{1}{r}\frac{\partial\psi}{\partial r}+\frac{1}{r^2}\frac{\partial^2\psi}{\partial\eta^2}+\frac{\partial^2\psi}{\partial z^2}\right)+\frac{ieH\hbar}{m^*c}\left(\cos\theta\frac{\partial\psi}{\partial\eta}+2r\sin\theta\sin\eta\frac{\partial\psi}{\partial z}\right)$$
$$+\frac{1}{2m^*}\left(\frac{2eH}{c}r\right)^2\left(\tfrac{1}{4}\cos^2\theta+\sin^2\theta\sin^2\eta\right)\psi=-\alpha\psi=E\psi , \tag{40}$$

where the azimuthal angle is measured from the direction defined by the external field, $\eta=\chi-\phi$.

This effective Schrödinger equation is rather complicated, but we can look for the energy eigenvalues using perturbation theory in the small field H near transition. Our unperturbed problem is

$$\frac{-\hbar^2}{2m^*}\left(\frac{\partial^2\psi}{\partial r^2}+\frac{1}{r}\frac{\partial\psi}{\partial r}+\frac{1}{r^2}\frac{\partial^2\psi}{\partial\eta^2}+\frac{\partial^2\psi}{\partial z^2}\right)=E^{(0)}\psi , \tag{41}$$

which is just the Helmholtz equation in cylindrical coordinates. The unperturbed eigenfunctions satisfying the boundary condition Eq. (39) are

$$\psi_{k_z ln}=e^{ik_z z}e^{il\eta}J_l(\bar{x}_{ln}/R) , \tag{42}$$

where $\bar{x}_{ln}$ is the nth zero of the first derivative of the lth Bessel function, corresponding to the energies

$$E_{k_z ln}=\frac{\hbar^2k_z^2}{2m^*}+\frac{\hbar^2}{2m^*}\left(\frac{\bar{x}_{ln}}{R}\right)^2 . \tag{43}$$

The lowest eigenvalue occurs for $k_z=0$ and $\bar{x}_{00}=0$. So to lowest order the order parameter is constant across the filament.

We now treat the potentials,

$$V_1=\frac{ie\hbar H}{m^*c}\left(\cos\theta\frac{\partial}{\partial\eta}+2r\sin\theta\sin\eta\frac{\partial}{\partial z}\right) ,$$

$$V_2=\frac{1}{2m^*}\left(\frac{2eH}{c}r\right)^2\left(\tfrac{1}{4}\cos^2\theta+\sin^2\theta\sin^2\eta\right) , \tag{44}$$

as perturbations. To second order in H the only contribution to the energy shift which survives is the diagonal matrix element of V_2 yielding

$$\Delta E_{000}^{(2)}=\frac{1}{2m^*}\left(\frac{eHR}{c}\right)^2\frac{1}{2}(1+\sin^2\theta) . \tag{45}$$

The second-order energy may be inverted to give the critical field

$$H_{c2}=\frac{\Phi_0}{\pi R\,\xi(0)}\left|\frac{T-T_c}{T_c}\right|^{1/2}\frac{2^{1/2}}{(1+\sin^2\theta)^{1/2}} . \tag{46}$$

The angular dependence of this isolated thin filament is much more gradual than the cusp at $\theta=0$ given by the corresponding formula due to Tinkam for thin films.[29,30] In the thin-film case, the normal vortex core can subsist within the film for a perpendicularly applied film but gets progressively "squeezed out" as the external field is made more parallel. This results in a divergence of $H_{c2\parallel}$ for a film of infinitesimal thickness. In the thin-filament case, the normal vortex core has been "squeezed out" for all orientations of the external field. Thus, in the limit $R\to 0$, critical fields for all angles are seen to diverge. Finally the temperature dependence of H_{c2} is given by

$$H_{c2}(T)/H_{c2}(0)=|T-T_c/T_c|^{1/2}$$

for all angles, and hence, exhibits downward curvature as the temperature is lowered, a result identical to the temperature dependence of $H_{c2\parallel}$ for thin films.

VI. PHYSICAL SYSTEMS

We briefly discuss in this section the application of the above theory to several physical systems. We first discuss the fibrous polymer $(SN)_x$ which provides an example of a coupled filamentary superconductor whose filaments tend to decouple as the temperature is lowered. We then speculate on the critical-field behavior of the transition-metal trichalcogenides $NbSe_3$ and $TaSe_3$, which appear to be filamentary on a microscopic scale, and which we also

expect to behave as coupled filamentary systems. Finally we comment on the critical-field measurements of isolated mercury filaments embedded in asbestos.

We first consider the pseudo-one-dimensional superconducting polymer $(Sn)_x$.[31–33] A Meissner state has been observed by Dee *et al.*[34] and although sample demagnetization effects preclude a definite identification of H_{c1} these workers have located the transition temperature at 0.23 °K for one of their samples. This is lower than the midpoint of the resistive transition but is similar to that observed in ac measurements.[35] Subsequent measurements[45] on other samples yield a transition temperature closer to that observed by the midpoint of the resistive transition. A Meissner state having been observed, we feel safe in applying our theory to this system.

The samples of $(SN)_x$ studied so far are highly fibrous with fiber diameters ranging from less than 100 Å, each fiber containing on the order of 100 polymer chains.[36] We apply the Ginzburg-Landau theory not to the individual chains of $(SN)_x$, but rather we treat the fibers as the filaments of the theory. The fibers are packed together, separated by only a few Å and are thus highly coupled near T_c. We will find a decoupling temperature T^* below which it will become necessary to incorporate the effect of finite fiber diameter. Clearly the theory should be improved to incorporate this effect of finite fiber diameter at all temperatures.

$(SN)_x$ has a physical transition temperature in the neighborhood of 0.3 °K (although as indicated above the actual value of T_c seems in dispute at present, depending both on sample and the type of measurement made), implying a Pauli paramagnetic limit[37,38] of

$$H_P = 18.4\,(\mathrm{kG/^\circ K})\,T_c = 5.4\ \mathrm{kG}\ .$$

This is exceeded by $H_{c2\parallel}$ for all temperatures below 0.18 °K, and a microscopic theory must be invoked in this regime. Qualitatively, the experimentally high critical fields might be understood on the basis of the decoupling of the filaments (due to a very large effective mass anisotropy), resulting in the divergence of the critical field in the Ginzburg-Landau theory. This divergence would be suppressed by taking into account the finite size of the filaments and by introducing various pair-breaking mechanisms, in particular Pauli paramagnetism. A crude microscopic calculation[39] for the dirty limit, neglecting crossed impurity averaging diagrams, gives rise to the usual pair-breaking equation; this exhibits Pauli limiting, which is violated in $(SN)_x$. Unlike the layered transition-metal dichalcogenide compounds, we do not expect spin-orbit scattering to play a significant role in $(SN)_x$. Thus, the violation of the Pauli limit must be attributed to another mechanism, such as the effect of flat portions of the Fermi surface driving the system[40,41] into the partially depaired Fulde-Ferrell state,[42] or perhaps this is an indication of triplet pairing.[43]

Assuming azimuthal isotropy, as initially indicated by Azevedo *et al.*,[5] the ratio

$$\left(\frac{dH_{c2\parallel}}{dT}\right)_{T_c} \Big/ \left(\frac{dH_{c2\perp}}{dT}\right)_{T_c} = \left(\frac{M}{m}\right)^{1/2}$$

implies an extremely large polar anisotropy. Using the data in Azevedo *et al.*[5] we deduce

$$\left(\frac{dH_{c2\parallel}}{dT}\right)_{T_c} = 7.29\times 10^4\,\mathrm{G/^\circ K}$$

and

$$\left(\frac{dH_{c2\perp}}{dT}\right)_{T_c} = 1.06\times 10^3\,\mathrm{G/^\circ K}$$

yielding a mass ratio $(M/m)^{1/2} = 68.9$, where we have taken $T_c = 0.285$ °K. This mass ratio is precisely the value $\epsilon^{-1} = H_{\parallel}/H_{\perp}$, cited in Azevedo *et al.*[5] near T_c. This mass ratio is consistent with the anisotropic mass polar dependence of H_{c2} at $T = 0.255$ °K (Fig. 5). The apparent decrease in the mass ratio as the temperature is lowered[5] might reflect some upward curvature of $H_{c2\perp}$ due to filament decoupling [Eq. (8)] (but as we shall see this is small) and certainly reflects the ultimate intervention of microscopic mechanisms which suppress $H_{c2\parallel}$ at the lower temperatures. With these critical-field slopes at T_c we compute, using Eq. (28) [or equivalently Eq. (7)] the $T = 0$ Ginzburg-Landau coherence lengths $\xi_\perp(0) = (m/M)^{1/2}\xi(0) = 126$ Å and $\xi_\parallel(0) = \xi(0) = 8680$ Å. The perpendicular coherence length is in agreement with Azevedo *et al.*[5] but the parallel coherence length is more than twice the value these authors compute from the same data. Their independent estimate[5] of the parallel coherence length from the 4 °K parallel resistivity yields a parallel coherence length of 3000 Å, in decided disagreement with the value obtained from taking the critical-field slopes at $T_c = 0.285$ °K. This value of T_c is also in disagreement with the ac measurements[35] and most importantly with the observation[34] of a Meissner effect at 0.23 °K.

Fixing $T_c = 0.23$ °K and using the data of Azevedo *et al.*[5] we fit

$$\left(\frac{dH_{c2\perp}}{dT}\right)_{T_c} = 3.38\times 10^3\,\mathrm{G/^\circ K}$$

unambiguously and

$$\left(\frac{dH_{c2\parallel}}{dT}\right)_{T_c} = 1.63\times 10^5\,\mathrm{G/^\circ K}\ .$$

This yields a mass ratio of 48.4 at T_c. The apparent

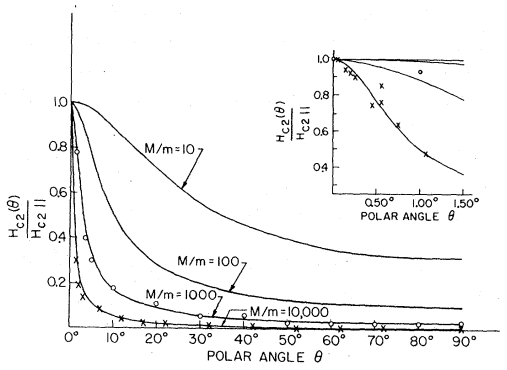

FIG. 5. Polar dependence of the critical field for various mass ratios $(M/m)^{1/2}$. Plotted also are the data points x for $(SN)_x$ at $T=0.255\,°K$ (Ref. 58) and the data points O for $TaSe_3$ at $T=1.73\,°K$ (Ref. 12).

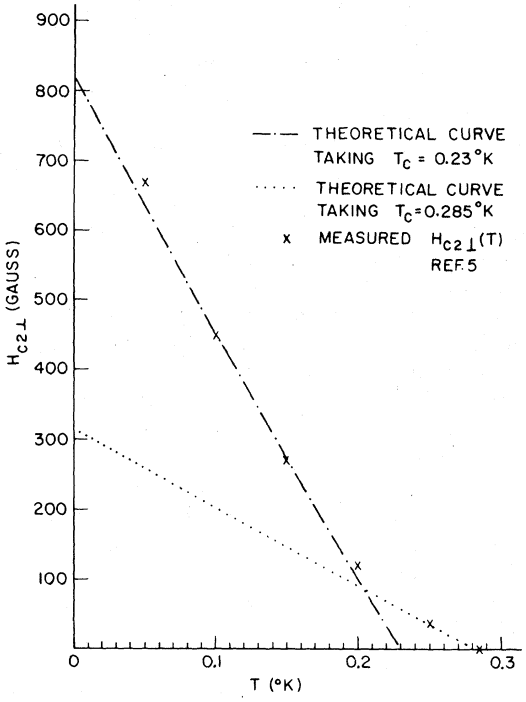

FIG. 6. Perpendicular upper critical-field $H_{c2\perp}$ for $(Sn)_x$. The theoretical curve taking $T_c=0.23\,°K$ cannot explain the significant superconductivity above 0.23 °K. The theoretical curve taking $T_c=0.285\,°$ K. cannot explain the significant upward curvature below 0.2 °K. The measured values are taken from Azevedo *et al.*[5].

decrease in the mass ratio as the temperature is lowered can then be ascribed solely to the Pauli limiting of $H_{c2\|}$ at these lower temperatures. (The new Pauli limit of 4.2 kG is exceeded at all temperatures below 0.2 °K.) The apparent increase in the mass ratio and indeed a presence at all of superconductivity for $T>0.23\,°K$ must be interpreted as being due to fluctuation conductivity. This would be corroborated by the conductivity measurements of Civiak *et al.*[44] in the absence of magnetic field, which they have fit to the Azlamazov-Larkin theory for one-dimensional fluctuation conductivity. (They obtain $T_c=0.255\,°K$ for their samples.) The presence of fluctuation conductivity over such a large temperature region is highly unusual, and that it is not suppressed by the parallel magnetic fields (of order kG) casts suspicion as to whether this mechanism is the source of the curvature in the $H_{c2\perp}$ curves. With these critical-field slopes at $T_c=0.23\,°K$ we compute the $T=0$ Ginzburg-Landau coherence lengths to be $\xi_\perp(0)=94$ Å and $\xi(0)=4530$ Å. The parallel coherence length now compares more favorably with the value 3300 Å, which we estimate from the 4 °K parallel resistivity. (This estimate has changed since T_c has been changed.) That T_c varies with different measurements and also seems to be sample dependent[45] makes $(SN)_x$ quite difficult to interpret theoretically.

The sudden increase of $H_{c2\|}$ near T_c opens the question of whether the filament coupling is so weak as to move T^* close to T_c. We now examine whether the filaments are still coupled at $T=0$. If they have already decoupled, then the polar dependence of H_{c2} should be given by Eq. (46). Furthermore, using $H_{c2\perp}$ at $T=0.05\,°K$ (which is not Pauli limited) generates a filament radius of 200 Å, which is too large.[36] We conclude that the filaments must still be coupled at $T=0$. (This conclusion is also reached using the parameters obtained fixing $T_c=0.285\,°K$.) We take as an upper bound a fiber diameter of 100 Å.[36] Since the fibers are observed to be packed closely together, we may use the fiber diameter as the fiber-fiber distance in our idealized model of infinitesimal filaments. Using Eq. (29) we compute the minimum extrusion of the $H_{c2\|}$ phase boundary to be $T_\|^{\min}=-0.06\,°K$, and using Eq. (10) the decoupling temperature to be $T^*=-0.58\,°K$. Averaging over azimuthal angles, Eqs. (8) and (9) become

$$H_{c2\perp}(T)=\frac{\Phi_0}{2\pi\xi_\perp(0)\xi_\|(0)}\left|\frac{T-T_c}{T_c}\right|\left\{1+\frac{3}{64}\frac{a^2}{\xi_\perp^2(0)}\left|\frac{T-T_c}{T_c}\right|+\frac{167}{24576}\frac{a^4}{\xi_\perp^4(0)}\left|\frac{T-T_c}{T_c}\right|^2+\cdots\right\} \quad (47)$$

Using $a = 100$ Å and $\xi_\perp^2(0) = 94$ Å we generate the temperature dependence of $H_{c2\perp}$ shown in Fig. 6. Shown also are the experimental values of $H_{c2\perp}$ taken from Azevedo *et al.*[5] The upward curvature at $T = 0$ is 5%. (Using $T_c = 0.285$ °K we compute the minimum extrusion of the $H_{c2\|}$ phase boundary to be $T_\|^{\min} = 0.35$ °K and the decoupling temperature to be $T^* = -1.52$ °K. This predicts a $T = 0$ value of $H_{c2\perp}$ of 315 G which is unacceptably low. For comparison the $H_{c2\perp}$ curve generated with this value of T_c is also shown in Fig. 6.)

In choosing $T_c = 0.23$ °K there is substantial disagreement of our model with the $H_{c2\|}(T)$ curve of Azevedo *et al.*[5] disagreement which cannot plausibly be attributed to fluctuation conductivity. (On the other hand, when we choose $T_c = 0.285$ °K our model agrees with the measured $H_{c2\|}(T)$ at T_c but only there, leaving unexplained the huge rise just below T_c.) With lattice spacing $a = 100$ Å we expect periodicity in the critical field every $\Phi_0/a^2 = 2 \times 10^5$ G. This is significantly beyond the Pauli limit, but with intercalation, the increased lattice size would reduce this periodicity scale. A possibility does exist, moreover, to observe the resonant bumps in the phase boundary due to fractional flux quanta being put through the unit cell of the filament lattice, although we expect that the periodic behavior in $H_{c2\|}$ will be smeared out due to any distribution in fiber sizes and any imperfections in the lattice of fibers. There is so far no evidence of any periodicity or quantized flux structure in the $H_{c2\|}$ data for $(SN)_x$. In fact $(SN)_x$ has been intercalated with bromine.[46,47] The bromine seems to increase the fiber-fiber coupling as seen in an increase in the temperature which locates the midpoint of the resistive transition. The low-field curvature in $H_{c2\perp}$ is also eliminated with intercalation,[46] and this supports the hypothesis that this curvature in the pure $(SN)_x$ may not be intrinsic. The increase in fiber-fiber coupling reduces the effective mass anisotropy, thereby suppressing the decoupling temperature. This undoes any advantage gained in increasing the lattice size, since the resonant bumps in the $H_{c2\|}$ phase boundary recede to lower temperatures as the decoupling temperature decreases. This effect could be exploited, however, if instead of intercalating with a material like bromine, which tends to enhance the fiber-fiber coupling, an intercalate which reduces the fiber-fiber coupling is introduced.

We now turn briefly to the transition-metal trichalcogenides. Monceau *et al.*[9,10] have reported a transition under pressure to the superconducting phase in $NbSe_3$. X-ray measurements[48] indicate a crystallographic structure of chains of trigonal prisms with chains relatively separated (Nb-Nb nearest-neighbor distances between chains is 4.25 Å). The anomalies in the resistivity at 145 and 59 °K have been interpreted as charge-density-wave transitions,[49,50] and recently have been observed as such,[51,52] and this supports an expectation of highly-one-dimensional characteristics in its superconducting properties. Under pressure, both of the charge-density-wave transitions occur at lower temperatures[53] indicating increased three-dimensional coupling. This is corroborated by a similar increase in the superconducting transition temperature under pressure.[9,10] Sambongi *et al.*[11] have similarly reported a transition to the superconducting phase in $TaSe_3$. The crystallographic structure as determined from x-ray measurements[54,55] is similar to that of $NbSe_3$ with a slightly larger unit cell. There are no resistive anomalies, and this together with the superconducting transition occurring at atmospheric pressure would indicate that $TaSe_3$ has stronger interchain coupling than $NbSe_3$.

Applying our model to these systems we expect the following qualitative behavior. Since the filament size is so small and the filament lattice is regular we expect that our model of coupled infinitesimal filaments will be more directly applicable to these systems than to $(SN)_x$. Since the coupling between the filaments is weak, we expect a very large anisotropic mass ratio which for $NbSe_3$ at least would be a strong function of pressure. This would yield decoupling temperatures which would also depend strongly on pressure. The weak coupling and small filament size will also make fluctuation effects more important in $NbSe_3$ than in $TaSe_3$. The intercalation of $NbSe_3$ with lithium[56] should allow an additional variation of both lattice size and interchain coupling, and intercalated systems analogous to the layered superconductors intercalated with organic molecules can presumably be made. Despite the regularity in the lattice for these systems [unlike $(SN)_x$], the small lattice size will preclude any observation of periodicity in the $H_{c2\|}$ phase boundary, but if the intercalated systems can be manufactured with sufficient crystal perfection, they might exhibit some of these $H_{c2\|}$ anomalies. Finally we should note the expected azimuthal anisotropy of the perpendicular critical field for these systems. Measurements by Monceau[57] of the Shubnikov–de Haas oscillations in $NbSe_3$ yield a ratio of 3 for the two cyclotron masses perpendicular to the chain direction (b axis). This would imply different filament couplings in the two directions leading to strong azimuthal dependence of $H_{c2\perp}$. This is borne out in the measurements of Sambongi *et al.*[13] for $H_{c2\perp}$ of $TaSe_3$ who find a cusp in the c direction implying very strong interfilament coupling in this direction. However, the interpretation of this result that $TaSe_3$ is microscopically two dimensional has the following difficulties. Using the Tinkham thin-film formula[29,30] yields a film thickness of 76 Å which incorporates several unit cells. In addition, one expects a similar cusp along the b axis where instead the anisotropic mass law is found to hold[12] with a mass ratio of $(M/m)^{1/2} = 30$ (see Fig. 5). A more complex model such as platelets of coupled filaments may

have to be invoked for these systems.

Finally, we comment briefly on the measurements of Bogomolov and coworkers. They have succeeded in manufacturing 20 Å filaments of mercury embedded in an asbestos matrix.[14] Their measurements of the critical field $H_{c2\|}$ indicate that the Pauli limit is exceeded by a factor of 3.[16] A microscopic theory would have to take into account the very real effect of spin-orbit scattering in this system. As the filaments are separated by 200–300 Å there should be no coupling between the filaments, and the treatment of Sec. V should be applicable. There should not be any upward curvature in the critical field, and indeed there is evidence of downward curvature, although the measurements as yet cannot establish the square-root dependence at T_c predicted by Eq. (46). The angular behavior of the critical field should be given by Eq. (46), and while this polar dependence has not been measured, the ratio $H_\perp/H_\|$ is essentially constant over the temperatures measured, consistent with Eq. (46).

ACKNOWLEDGMENTS

We are grateful to L.J. Azevdo and R. L. Greene for kindly sending us their unpublished measurements of the polar dependence of $H_{c2\|}$ for $(SN)_x$ at 0.255 °K (Fig. 5) and for several invaluable discussions. We are grateful to M. Yamamoto for sending us his unpublished measurements of the polar dependence of H_{c2} for $TaSe_3$ at 1.73 °K (Fig. 5). We would like to thank S. Doniach, W. A. Little, R. H. Dee, W. G. Clark, and W. Dieterich for fruitful discussions and also the latter for bring to our attention the work of Manneville (Ref. 7). We thank the Danforth Foundation (L.A.T.), the U.S. DOE, Division of Basic Energy Sciences (R.A.K.), and the Army Research Office, Durham, North Carolina for their support.

APPENDIX A: EXACT SOLUTIONS OF $H_{c2\perp}(T)$ FOR $\phi = 0, \frac{1}{4}\pi$

Two special cases of the eigenvalue equation (5), which determines $H_{c2\perp}(T)$, may be solved exactly, and we treat these special cases in this Appendix. For simplicity we take the system to have isotropic coupling ($\zeta_x = \zeta_y = \zeta$; $a = b$).

For azimuthal angle $\phi = 0$ (or $\phi = \frac{1}{2}\pi$) the eigenvalue equation (5) reduces to the Mathieu equation

$$\frac{d^2\psi}{dx^2} + \frac{1}{h^2}\frac{a^2}{\xi^2(0)}\frac{T_0^* - T}{T_c}\psi + 2\frac{m}{M}\frac{1}{h}\cos 2x\,\psi = 0 \ , \tag{A1}$$

where we have set $x = hz/a$ and where

$$T_0^*/T_c = 1 - 2[m\xi^2(0)/Ma^2] \ .$$

Similarly for azimuthal angle $\phi = \frac{1}{4}\pi$ the eigenvalue equation (5) reduces to the Mathieu equation

$$\frac{d^2\psi}{dx^2} + \frac{1}{h^2}\frac{2a^2}{\xi^2(0)}\frac{T^* - T}{T_c}\psi + 2\frac{4m}{M}\frac{1}{h^2}\cos 2x\,\psi = 0 \ , \tag{A2}$$

where we have set $x = hz/a\,(2)^{1/2}$ and where

$$T^*/T_c = 1 - 4[m\xi^2(0)/Ma^2] \ .$$

Inverting the lowest Mathieu eigenvalue in the large parameter expansion[27] yields the critical-field behavior near T_c

$$H_{c2\perp} = \frac{\Phi_0}{2\pi a^2}\left(\frac{m}{M}\right)^{1/2}\sum_{n=1}^{\infty} c_n\left(\frac{a}{\xi_\perp}(0)\right)^{2n}\left|\frac{T_c - T}{T_c}\right|^n \ , \tag{A3}$$

with

$$\begin{aligned}
&c_1(0) = 1, && c_1(\tfrac{1}{4}\pi) = 1 \ , \\
&c_2(0) = 1/2^4, && c_2(\tfrac{1}{4}\pi) = 1/2^5 \ , \\
&c_3(0) = 3/2^8, && c_3(\tfrac{1}{4}\pi) = 3/2^{10} \ , \\
&c_4(0) = 13/2^{12}, && c_4(\tfrac{1}{4}\pi) = 13/2^{15} \ , \\
&c_5(0) = 2293/2^{22}, && c_5(\tfrac{1}{4}\pi) = 2293/2^{26} \ .
\end{aligned} \tag{A4}$$

Inverting the lowest-Mathieu eigenvalue in the small parameter expansion[20] yields the divergent critical-field behavior near T_0^* (for $\phi = 0$) and near T^* (for $\phi = \frac{1}{4}\pi$). We have

$$H_{c2\perp}(0) = \frac{\Phi_0}{\pi a^2}\frac{1}{2^{1/2}}\frac{m}{M}\frac{\xi(0)}{a}\left(\frac{T_c}{T - T_0^*}\right)^{1/2}\left[1 - \tfrac{1}{2}\sum_{m=1}^{\infty} a_{2m+1}\left(\frac{a}{\xi_\perp(0)}\right)^{2m}\left(\frac{T_0^* - T}{T_c}\right)^{2m}\right]^{-1/2} \ , \tag{A5}$$

where

$$a_3 = -\tfrac{7}{8}, \quad a_5 = \frac{3565}{1152}, \quad a_7 = \frac{58625}{73728} \ , \tag{A6}$$

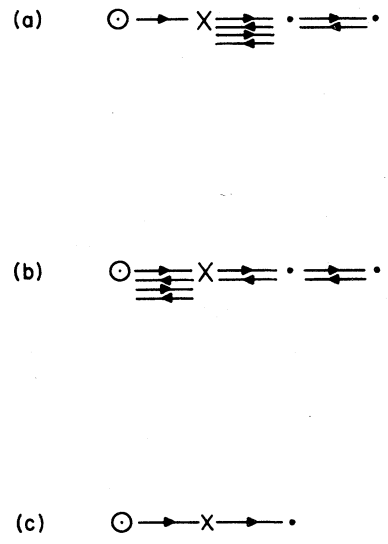

FIG. 7. Acceptable (a) and unacceptable (b) and (c) walks for the one-term Hill (i.e., Mathieu) eigenvalue equation.

and we have

$$H_{c2\perp}(\tfrac{1}{4}\pi)=\frac{\Phi_0}{\pi a^2}\frac{1}{2^{1/2}}\frac{2m}{M}\frac{\xi(0)}{a}\left(\frac{T_c}{T-T^*}\right)^{1/2}\times\left[1-\sum_{m=1}^{\infty}b_{2m+1}\left(\frac{a}{\xi_\perp(0)}\right)^{2m}\left(\frac{T^*-T}{T_c}\right)^{2m}\right]^{-1/2}, \tag{A7}$$

with eigenvalue

$$\bar{\sigma}^2=\left(\frac{\sigma^2+2\lambda^2\sigma_m^2}{4m^2}\right)\Big/n^2\left(1-\frac{3\lambda^2\sigma_m^2}{8m^4}\right)^{-1} \tag{A10}$$

and parameter

$$\bar{\lambda}=\lambda\sigma_n/n^2\left(1-\frac{3\lambda^2\sigma_m^2}{8m^4}\right)^{-1}.$$

Utilizing the well-known large parameter expansion[27] for the Mathieu eigenvalues, and working only to lowest order in $\sin\phi$ (since we are interested in the behavior as $\phi\to 0$), we obtain for isotropic coupling (with $\bar{h}=(m/M)^{1/2}h$),

where

$$b_3=-\frac{7}{64},\quad b_5=\frac{3565}{36864},\quad b_7=\frac{58625}{9437184}. \tag{A8}$$

These critical fields are graphed in Fig. 3 with an interpolation between the high- and low-field expansions. There is upward curvature to these critical fields, but this only becomes significant in the vicinity of $T_0{}^*$ (for $\phi=0$) and T^* (for $\phi=\frac{1}{4}\pi$); near T_c the critical-field curve is very linear.

APPENDIX B: $H_{c2\perp}$ NEAR $\phi=0$

In this Appendix we examine the azimuthal dependence of $H_{c2\perp}$ near the "singular" angle $\phi=0$ (and similarly near $\phi=\frac{1}{2}\pi$). As we let $\phi\to 0$ (i.e., $n_y\to 0$), the high-field expansion (18) contains divergent terms to all orders in λ. In Appendix C a diagrammatic representation for each term of Eq. (18) is constructed, and this diagrammatic representation facilitates a summation of the divergent terms, yielding the well-known[26] continued-fraction equation for the Mathieu eigenvalues

$$\bar{\sigma}^2+\cfrac{2\bar{\lambda}^2}{4n^2-\bar{\sigma}^2-\cfrac{\bar{\lambda}^2}{16n^2-\bar{\sigma}^2-\cfrac{\bar{\lambda}^2}{36n^2-\bar{\sigma}^2-\cdots}}}=0, \tag{A9}$$

$$\frac{1}{\bar{h}^3}-2\frac{1}{\bar{h}}\frac{\alpha+2\zeta}{\zeta}-4\sin\phi\left(1-\frac{3}{8\bar{h}^4}\right)^{1/2}=0, \tag{A11}$$

where $\bar{h}=(m/M)^{1/2}h$. The singularity at $\phi=0$ manifests itself in the change in order of this eigenvalue equation, and this leads to the strong azimuthal dependence at low temperatures near $\phi=0$. This is graphically displayed in Fig. 3.

APPENDIX C: DIAGRAMMATIC ANALYSIS OF HILL EIGENVALUE EQUATIONS

In this Appendix we develop a diagrammatic analysis of the eigenvalue equation for the Hill dif-

ferential equation. A general (N-term) Hill equation will be of the form

$$\frac{d^2\psi}{dx^2}+\sigma^2\psi+2\lambda\sum_{l=1}^{N}\sigma_{n_l}\cos(2n_lx)\psi=0 \quad . \tag{A12}$$

This has eigenvalues determined from the equation[21]

$$\sigma^2+\sum_{\{\kappa_l\}}\lambda^{j+1}\frac{\sigma_{|\kappa_1|}\sigma_{|\kappa_2|}\cdots\sigma_{|\kappa_j|}\sigma_{|\kappa_1+\cdots+\kappa_j|}}{[(2\kappa_1+\tau)^2-\sigma^2][(2\kappa_1+2\kappa_2+\tau)^2-\sigma^2]\cdots[(2\kappa_1+2\kappa_2+\cdots 2\kappa_j+\tau)^2-\sigma^2]}=0 \quad , \tag{A13}$$

where the sum is over all $\kappa=\pm n_l$ subject to the restrictions $\kappa_1+\cdots+\kappa_j=\pm n_l$ and $\kappa_1+\cdots+\kappa_i\neq 0$ for all $i<j$.

To each term in the sum (A13) we may associate a walk on an N-dimensional Cartesian lattice, starting at the origin 0, thereafter avoiding the origin, and ending one step away from the origin at X with only unit steps permitted in the Cartesian directions. For each step in the l direction we pick up a factor $\lambda\sigma_{|n_l|}$. For each step ending at site $\sum_{l=1}^{N}s_ln_l$ (with integer s_l) we pick up a factor

$$\left[\left(2\sum_{l=1}^{N}s_ln_l+\tau\right)^2-\sigma^2\right]^{-1} \quad .$$

Finally, for the end point of the walk, which will be at some $\pm n_l$, we associate a factor $\lambda\sigma_{|n_l|}$.

If some of the numbers n_l are commensurate, then some linear combination of the n_l with integer coefficients will vanish, and hence these correspond to lattice sites "equivalent" to the origin. These lattice sites must also be avoided in any acceptable lattice walk. The nearest neighbors of these equivalent origins are equivalent end points, and are possible end points for acceptable lattice walks.

For simplicity, we treat only the case $\tau=0$ in this analysis.

1. *Mathieu equation*

In this subsection we treat the Mathieu equation which is just the one-term Hill equation

$$\frac{d^2\psi}{dx^2}+\sigma^2\psi+2\lambda\cos 2nx\,\psi=0 \quad . \tag{A14}$$

Each term of the sum in the eigenvalue equation (A13) may be represented by a walk on a one-dimensional lattice, starting at the origin, thereafter avoiding the origin, and ending one step away from the origin. As an example, Fig. 7(a) is an acceptable walk corresponding to the term

$$\lambda^8(4n^2-\sigma^2)^{-3}(16n^2-\sigma^2)^{-3}(36n^2-\sigma^2)^{-1} \quad .$$

However Fig. 7(b) is not an acceptable walk since it returns to the origin; neither is Fig. 7(c) an acceptable walk since it does not end at a point one step away from the origin.

We now proceed to a summation of all classes of such walks, thereby deriving the Mathieu eigenvalue equation:

(i) All walks start with either a step to the left or one to the right. By overall multiplication by 2 we can include all walks starting to the left. Each walk will thus carry a factor $2\lambda(4n^2-\sigma^2)^{-1}$ which may be pulled out as a multiplicative factor.

(ii) Summing all walks going only one step away from the end point X yields $\Sigma^{(1)}/(1-\Sigma^{(1)})$, where we have

$$\Sigma^{(1)}=\frac{\lambda^2}{[(4n^2-\sigma^2)(16n^2-\sigma^2)]} \quad . \tag{A15}$$

This is depicted diagrammatically in Fig. 8.

All walks going at most one step away from the end point X thus sum to $1/(1-\Sigma^{(1)})$.

(iii) Summing all walks going only two steps away from the end point X with only one traversal through X yields $\Sigma^{(2)}$ with

$$\Sigma^{(2)}=\frac{\lambda^2}{(4n^2-\sigma^2)(16n^2-\sigma^2)}\,\frac{\dfrac{\lambda^2}{(16n^2-\sigma^2)(36n^2-\sigma^2)}}{1-\dfrac{\lambda^2}{(16n^2-\sigma^2)(36^2-\sigma^2)}} \quad . \tag{A16}$$

This is depicted diagrammatically in Fig. 9.

(iv) Summing all walks going at most two steps away from the end point X with any number of traversals through X yields

$$\frac{1}{1-\Sigma^{(1)}}\left[1+\Sigma^{(2)}\frac{1}{1-\Sigma^{(1)}}+\left(\Sigma^{(2)}\frac{1}{1-\Sigma^{(1)}}\right)^2+\cdots\right]=\frac{1}{1-\Sigma^{(1)}}\left(1-\frac{\Sigma^{(2)}}{1-\Sigma^{(1)}}\right)^{-1}=\frac{1}{1-\Sigma^{(1)}-\Sigma^{(2)}} \quad . \tag{A17}$$

To this order the eigenvalue equation is

$$\sigma^2+\frac{2\lambda^2}{4n^2-\sigma^2}\frac{1}{1-\Sigma^{(1)}-\Sigma^{(2)}}=\sigma^2+\cfrac{2\lambda^2}{4n^2-\sigma^2-\cfrac{\lambda^2}{16n^2-\sigma^2-\cfrac{\lambda^2}{36n^2-\sigma^2}}}=0 \quad . \tag{A18}$$

This is just the third convergent of the Mathieu eigenvalue equation.[26] As the walk summation is a recursive procedure on the one-dimensional lattice it should be clear that summation of third- and higher-order walks will generate the higher-order convergents of this continued-fraction equation.

2. *Two-term Hill equation*

In this subsection we treat the two-term Hill equation

$$\frac{d^2\psi}{dx^2}+\sigma^2+2\lambda(\sigma_m\cos 2mx+\sigma_n\cos 2nx)\psi=0 \quad . \tag{A19}$$

Each term of the eigenvalue equation (A13) may be represented by a walk on a two-dimensional lattice, starting at the origin, and ending one step away from the origin, with care taken to avoid equivalent origins, although a walk may end at an equivalent end point. We will label horizontal walks as n walks and vertical walks as m walks. As an example, the walk in Fig. 10 is an acceptable walk corresponding to the term

$$\lambda^6\sigma_n^4\sigma_m^2(4n^2-\sigma^2)^{-1}[4(n+m)-\sigma^2]^{-1}\times[4(2n+m)^2-\sigma^2]^{-1}[4(2n)^2-\sigma^2]^{-1} \quad .$$

With the advent of the second dimension, the task of classifying and summing all walks is made considerably more difficult. In two cases the topology reduces to one dimension as it should. When $n=0$ all strictly horizontal points become equivalent origins as in Fig. 11(a). All of the walks may be summed to yield $\sigma^2+2\lambda\sigma_n$ as the Mathieu eigenvalue

$$(\sigma^2+2\lambda\sigma_n)+\cfrac{2\lambda^2\sigma_m^2}{4m^2-(\sigma^2+2\lambda\sigma_n)-\cfrac{\lambda^2\sigma_m^2}{16m^2-(\sigma^2+2\lambda\sigma_n)+\cdots}}=0 \quad . \tag{A20}$$

Similarly when $n\rightarrow m$ all upper-left and lower-right strict diagonal sites become equivalent origins as in Fig. 11(b). All of the walks may be summed to yield σ^2 as the Mathieu eigenvalue

$$\sigma^2+\cfrac{2\lambda^2(\sigma_m+\sigma_n)^2}{4m^2-\sigma^2-\cfrac{(\sigma_m+\sigma_n)^2}{16m^2-\sigma^2-\cdots}}=0 \quad . \tag{A21}$$

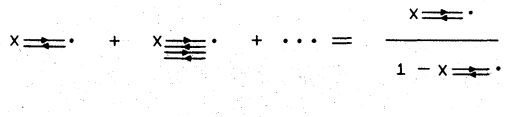

FIG. 8. Summation of the one-step walks for the Mathieu eigenvalue.

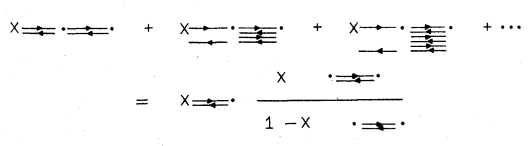

FIG. 9. Summation of the two-step walks with only one traversal of the end point for the Mathieu eigenvalue.

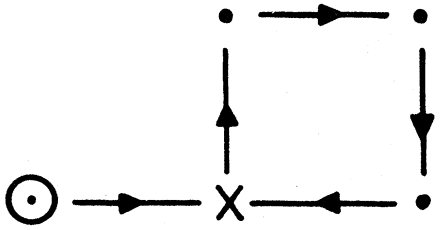

FIG. 10. An acceptable walk for the two-term Hill eigenvalue equation.

3. *Approximation of the two-term Hill equation eigenvalue*

We now approximate the eigenvalue for the two-term Hill equation (A19) as the parameter $n \to 0$. The treatment of the two-term Hill equation in Sec. C 2 indicates one must sum an infinite class of walks. In other words, an infinite number of terms in the expression (A13) of the secular determinant have vanishing demoninator. Clearly all walks which never stray from the horizontal will involve only n in the denominators and hence will be singular; we must sum all of these walks, and as $n \to 0$, this sum yields the continued-fraction equation (A20). Working to lowest nontrivial order, we sum all walks which stray only one vertical step away from the horizontal. These terms are nonsingular as $n \to 0$ and at least of order λ^2. Including walks straying further from the horizontal would keep terms of higher order in λ, even as $n \to 0$. Thus, to order λ^2, the behavior of the eigenvalue as $n \to 0$ is represented by all walks within one step of the horizontal on the two-dimensional lattice. Summing these walks yields the continued-fraction equation

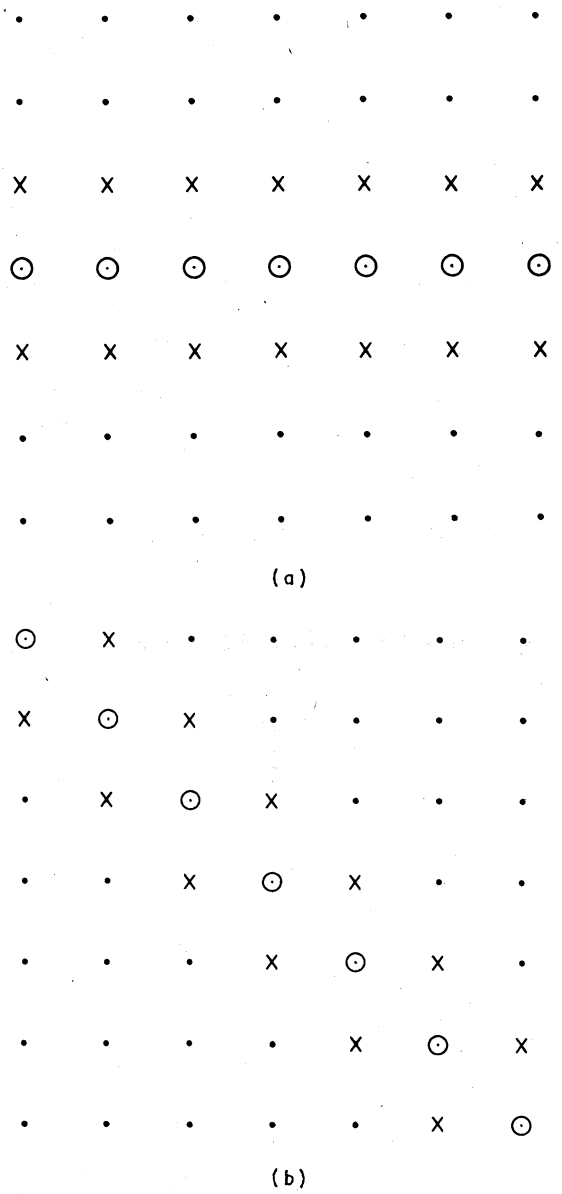

FIG. 11. Equivalent origins and equivalent end points (a) as $n \to 0$ and (b) as $n \to m$.

$$\sigma^2+\frac{2\lambda^2\sigma_m^2}{4m^2}+2\lambda^2\sigma_n^2\left(\sigma^2-4n^2+\frac{\lambda^2\sigma_m^2}{4(n+m)^2}+\frac{\lambda^2\sigma_m^2}{4(n-m)^2}-\frac{\lambda^2\sigma_n^2}{\sigma^2-4(2n)^2+\cdots}\right)^{-1}=0\ . \tag{A22}$$

Since we are interested in the limit $n \to 0$ we may expand the denominators

$$(m\pm n)^{-2}=m^{-2}[1\mp 2n/m+3(n/m)^2+\cdots]\ ,$$

This yields the continued fraction for the Mathieu eigenvalue

$$\bar{\sigma}^2 + \cfrac{2\bar{\lambda}^2}{4n^2 - \bar{\sigma}^2 - \cfrac{\bar{\lambda}^2}{16n^2 - \bar{\sigma}^2 - \cfrac{\bar{\lambda}^2}{36n^2 - \bar{\sigma}^2 - \cdots}}}} = 0 \ . \tag{A23}$$

where

$$\bar{\sigma}^2 = \left(\sigma^2 + \frac{2\lambda^2\sigma_m^2}{4m^2}\right) \Big/ n^2\left(1 - 3\frac{\lambda^2\sigma_m^2}{8m^4}\right)^{-1} , \qquad \bar{\lambda} = \lambda\sigma_n / n^2\left(1 - 3\frac{\lambda^2\sigma_m^2}{8m^4}\right) , \tag{A24}$$

which is the result [Eq. (A9)] used in Appendix B.

*Present address: Dept. of Phys., Univ. of Calif., Los Angeles, Calif. 90024.

[1]W. A. Little, Phys. Rev. A 134, 1416 (1964).
[2]D. Davis, H. Gutfreund, and W. A. Little, Phys. Rev. B 13, 4766 (1976).
[3]H. Gutfreund and W. A. Little, in *NATO Advanced Institute in Chemistry and Physics of One-Dimensional Metals, Bolzano 1976,* edited by H. J. Keller (Plenum, New York, 1977), p. 279.
[4]R. L. Greene, G. B. Street, and L. J. Suter, Phys. Rev. Lett. 34, 577 (1975).
[5]L. J. Azevedo, W. G. Clark, G. Deutscher, R. L. Greene, G. B. Street, and L. J. Suter, Solid State Commun. 19, 197 (1976).
[6]W. Lawrence and S. Doniach, in *Proceedings of the 12th International Conference on Low Temperature* Physics, edited by Eizo Kanda (Academic, Kyoto, 1971), p. 361.
[7]P. Manneville, J. Phys. (Paris) 36, 701 (1975).
[8]L. A. Turkevich, Bull. Am. Phys. Soc. 22, 371 (1977).
[9]P. Monceau, J. Peyrard, and J. Richard, Bull. Am. Phys. Soc. 22, 403 (1977).
[10]P. Monceau, J. Peyrard, J. Richard, and P. Molinie, Phys. Rev. Lett. 39, 161 (1977).
[11]T. Sambongi, M. Yamamoto, K. Tsutsumi, Y. Shiozaki, K. Yamaya, and Y. Abe, J. Phys. Soc. Jpn. 42, 1421 (1977).
[12]M. Yamamoto, thesis (unpublished).
[13]T. Sambongi, Kotai Butsuri (Solid State Phys.) 12, 545 (1977) (in Japanese).
[14]V. N. Bogomolov and Yu. A. Kumzerov, JETP Lett. 21, 198 (1975).
[15]V. N. Bogomolov and V. K. Krivosheev, Sov. Phys. Solid State 13, 672 (1971).
[16]V. N. Bogomolov, N. A. Klushin, Yu. A. Kumzerov, and P. A. Cheremnykh, Sov. Phys. Solid State 18, 858 (1976).
[17]V. N. Bogomolov and V. I. Krivosheev, Sov. Phys. Solid State 14, 1059 (1972).
[18]R. A. Klemm, A. Luther, and M. R. Beasley, Phys. Rev. B 12, 877 (1975).
[19]M. Tinkham, *Introduction to Superconductivity* (McGraw-Hill, New York, 1975), p. 124, Eq. 4.51.
[20]N. W. McLachlan, *Theory and Application of Mathieu Functions* (Dover, New York, 1964), p. 15, Eq. 2.150-7 .
[21]M. Golomb, Arch. Rat. Mech. Anal. 2, 284 (1958-9).
[22]E. T. Whittaker and G. N. Watson, *A Course of Modern Analysis* (Cambridge University, Cambridge, 1946), Sec. 19.12.
[23]M. S. P. Eastham, *The Spectral Theory of Periodic Differential Equations* (Scottish Academic, Edinburgh, 1973), Chap. 1.
[24]W. Magnus and W. Winkler, *Hill's Equation* (Interscience, New York, 1966).
25 T. Fort, *Finite Differences and Difference Equations in the Real Domain* (Oxford University, Oxford, 1948), p. 178
[26]N. W. McLachlan, see Ref. 20, p. 29, Eq. 3.11-8.
[27]N. W. McLachlan, see Ref. 20, p. 232, Eq. 11.44-1.
[28]D. Saint-James and G. Sarma, *Type II Superconductivity* (Pergamon, Oxford, 1963), Part I, Sec. 4.3.
[29]M. Tinkham, see Ref. 19, p. 134, Eq. 4-70.
[30]M. Tinkham, Phys. Rev. 129, 2413 (1963).
[31]R. L. Greene and G. B. Street, see Ref. 3, p. 167.
[32]G. B. Street and R. L. Greene, IBM J. Res. Dev. 21, 99 (1977).
[33]H. P. Geserich and L. Pintschovius, in *Festkorperprobleme (Advances in Solid State Physics),* edited by J. Treusch (Braunschweig 1976), Vol. XVI, p. 165.
[34]R. H. Dee, D. H. Dollard, B. G. Turrell, and J. F. Carolan, Solid State Commun. 24, 469 (1977).
[35]R. H. Dee, A. J. Berlinsky, J. F. Carolan, E. Klein, N. J. Stone, and B. G. Turrell, Solid State Commun. 22, 303 (1977).
[36]L. R. Bickford, R. L. Greene, and W. D. Gill (to be published).
[37]B. S. Chandrasekhar, Appl. Phys. Lett. 1, 7 (1962).
[38]A. M. Clogston, Phys. Rev. Lett. 9, 266 (1962).
[39]K. Machida and R. A. Klemm (private communication).
[40]K. Aoi, W. Dieterich, and P. Fulde, Z. Phys. 267, 223 (1974).
[41]L. N. Bulaevskii, Zh. Eksp. Teor. Fiz. 65, 1278 (1975).
[42]P. Fulde and R. A. Ferrel, Phys. Rev. A 135, 550 (1974).
[43]K. Machida and R. A. Klemm, Solid State Commun. (to be published).
[44]R. L. Civiak, C. Elbaum, W. Junker, C. Gough, H. I. Kao, L. F. Nichols, and M. M. Labes, Solid State Commun. 18, 1205 (1976).
[45]R. H. Dee (private communication).
[46]J. F. Kwak, R. L. Greene, and G. B. Street, Bull. Am.

Phys. Soc. 23, 384 (1978).
[47]R. H. Dee, D. H. Dollard, J. F. Carolan, B. G. Turrell, R. L. Greene, and G. B. Street, Bull. Am. Phys. Soc. 23, 384 (1978).
[48]A. Meerschaut and J. Rouxel, J. Less Common Metals 39, 197 (1975).
[49]P. Monceau, N. P. Ong, A. M. Portis, A. Meerschaut, and J. Rouxel, Phys. Rev. Lett. 37, 602 (1976).
[50]J. Chaussy, P. Haen, J. C. Lasjaunias, P. Monceau, G. Waysand, A. Waintal, A. Meerschaut, P. Molinie, and J. Rouxel, Solid State Commun. 20, 759 (1976).
[51]K. Tsutsumi, T. Takagaki, M. Yamamoto, Y. Shiozaki, M. Ido, T. Sambongi, K. Yamaya, and T. Abe, Phys. Rev. Lett. 39, 1675 (1977).
[52]R. M. Fleming, D. E. Moncton, and D. B. McWhan, Bull. Am. Phys. Soc. 23, 425 (1978).
[53]P. Haen, G. Waysand, G. Boch, A. Waintal, P. Monceau, N. P. Ong, and A. M. Portis, J. Phys. Coll. 37, C4-179 (1976).
[54]E. Bjerkelund and A. Kjekshus, Acta Chem. Scand. 19, 701 (1965).
[55]E. Bjerkelund, J. H. Fermor, and A. Kjekshus, Acta Chem. Scand. 20, 1836 (1966).
[56]D. Murphy (private communication).
[57]P. Monceau, Solid State Commun. 24, 331 (1977).
[58]L. J. Azevedo and R. L. Greene (unpublished).